THERMAL AND MICROSTRUCTURAL ANALYSIS OF THE LOW-MELTING Bi–In–Sn TERNARY ALLOYS

Ljubiša Balanović, Dragan Manasijević, Ivana Marković, Milan Gorgievski, Uroš Stamenković,
University of Belgrade, Technical Faculty in Bor
Bor, Serbia

Dajana Milkić
Measuring Transformers Factory Zaječar (FMT Zaječar)
Zaječar, Serbia

Keywords: Bi-In-Sn alloys, differential thermal analysis (DTA), microstructure, SEM-EDS

ABSTRACT
Low-melting alloys, based on bismuth, indium, and tin, have found commercial use in soldering, safety devices, coatings, and bonding applications, due to their low melting point temperature of eutectic compositions and small differences between their liquidus and solidus temperatures. Based on this, the accurate knowledge of their thermal properties such as melting and solidification temperatures, latent heat of melting, supercooling tendency, etc. is of immense importance. In the present research, low-melting alloy from three cross-sections Bi-Sn50In50, Sn-In50Bi50, and In-Bi50Sn50 (wt.%) was investigated using differential thermal analysis (DTA), and by scanning electron microscopy (SEM) with energy dispersive spectrometry (EDS). Temperatures of phase transformations, determined by DTA, and phase compositions of co-existing phases, determined by EDS analysis, were found to support the corresponding calculated phase compositions quite well. The experimentally obtained results were compared with the results of thermodynamic calculation according to the CALPHAD approach, and a close agreement was noticed.

1. INTRODUCTION

Solders known as fusible metal or material become an important element since it will ensure the continuity of the production of electrical and mechanical in the electronic packaging [1]. As is known to all, Tin-Lead (Sn-Pb) solders have been used for many years due to their good chemical, physical, thermal, and mechanical properties as traditional solders in the field of electronic packaging [2]. However, concerning the toxicity of Pb to human health and the environment, many countries have limited or banned the production and application of Sn-Pb solders in many fields by means of legislation [3,4]. For example, the implementation of WEEE directives [5] and RoHS [6-8] regulations in the national legislation of the European Union, the USA, and Japan lasted until January 2, 2013. Since consumer needs for electronic devices are increasing every day, the need for new lead-free alloys that are suitable for soldering is also increasing [9]. The Sn-Bi base lead-free solders are proposed as one of the most popular alloys due to the low melting temperature (eutectic point: 139^{O}C) and low cost. However, they are not widely used because of the lower wettability, fatigue resistance, and elongation compared to traditional Sn-Pb solders. So alloying is considered an effective way to improve the properties of Sn-Bi solders with the addition of elements Al, Cu, Zn, Ga, Ag, Sb, as well as indium [10]. The alloy from Bi-In-Sn system was investigated by

Noor et al. [9], as a potential candidate to replace Tin-Lead (Sn-Pb) solders. That alloy gives a low melting temperature in the range of 65-100 ℃, which is directly contributed by the addition of In. The lowest melting temperature ensures that the solder melts and forms a joint with the substrates, after which it solidifies again in the shortest period. The melting temperature of the alloy from the Bi-In-Sn system is about 60℃ because In and Bi have the ability to effectively reduce the melting temperature of the solder. Based on this study, it was concluded that according to the microstructure analysis, the presence of the intermetallic compound BiIn can be observed for the solder with the Bi-In-Sn system. Recently, Zhou et al [11] investigated the microstructure, phase morphology, temperature, and heat of the fusion of several alloys from the Bi-In-Sn system. The examination was carried out by scanning electron microscopy (SEM) with energy dispersive spectrometry (EDS), X-ray diffraction (XRD), differential scanning calorimetry (DSC), and a density analysis instrument. Based on the obtained results, it was concluded that the alloys have an extremely low melting point as well as a high density [11]. Yang et al. [12] performed a thermodynamic calculation using the CALPHAD method, as well as corresponding experiments to design low-temperature Bi-In-Sn solders. They concluded that when it comes to the mechanical characteristics of the solder, during air cooling, a large relaxation limit of the solder, high tensile strength, and much better elongation are obtained than the conventional solder. The Bi-Sn system has a low melting point. In order to improve the mechanical characteristics of the Bi-Sn solder, In was added and they obtained a better elongation of the solder, thus maintaining a low melting temperature. Shalaby et al. [13] found that the addition of In elements had a critical effect on the onset point of the Sn-58Bi solder which meant that adding 2 wt.% In could decrease the onset point of the solder from 139.06°C to 129.68°C and increase the tensile and shear strength. Chen et al. [14] studied the effects of In addition on the melting temperature and tensile properties of Sn-Bi solder. When the content of In addition was 5 wt.%, the onset point was decreased by about 20°C, and tensile properties were poor decreasing from 71.8 MPa to 68.3 MPa when the content of the, In addition, was at 3 wt.%. With increasing In content, the peak temperature of the composite solder was reduced by 10°C. The most important thermodynamic optimization of the Bi-In-Sn system, which is based on new experimental data, was carried out by Witusiewicz et al. [15]. A new thermodynamic description is presented for the ternary Bi-In-Sn system in the entire range of compositions. The parameters for the thermodynamic models of the constituent binary systems Bi-In, Bi-Sn, and In-Sn were adopted from earlier research, and those for the system Bi-In-Sn were optimized using experimental data on phase equilibria as well as data on melting enthalpy of different alloys available in the literature. In the present research, low-melting alloy from three cross-sections Bi-Sn50In50, Sn-In50Bi50, and In-Bi50Sn50 was investigated using differential thermal analysis (DTA), and by scanning electron microscopy (SEM) with energy dispersive spectrometry (EDS). Although there are numerous studies of the thermal and structural characteristics, the Bi-In-Sn ternary system is still in the research phase.

2. EXPERIMENTAL PROCEDURE

Sample preparation in the present study consisted in melting the raw metals Bi, In, and Sn with a purity of 99.999 mass%, in an induction furnace under a protective argon atmosphere. The melting procedure involved heating the samples together with the furnace for about 90 min, to the temperature of 100 °C above the liquidus line, keeping them at that temperature for 60 minutes to ensure the homogenization of the molten alloy, and slowly cooling inside the furnace. Then, the samples were annealed at 100 °C for three hours in order to eliminate internal stresses and additional homogenization. The

total mass of the prepared sample was about 4 g, while the total mass loss was less than 1 mass%. Phase transition temperatures and corresponding heat effects were determined by a simultaneous thermal analyzer (TA Instruments SDT Q600) [16]. The reference material was an empty alumina crucible. Prior to DTA measurements, temperature and enthalpy calibrations were performed using pure metal standards (In and Zn) under the measurement conditions. The sample's masses were about 30 mg and each sample was investigated by performing two heating cycles using the heating rate of 10 °C/min in the temperature interval from room temperature up to 300 °C, in a stream of inert gas (nitrogen) to prevent oxidation of the sample. Scanning electron microscope (SEM) (TESCAN VEGA3) [17], with an energy dispersive spectrometer (EDS) (Oxford Instruments X-act) [18], was used for microstructural investigation of the prepared alloys. The compositions of the coexisting phases as well as the total composition of the prepared alloys were determined using surface and spot EDS analysis. All SEM images of microstructures were recorded in the backscattered electron mode [17]. The analyzed samples were prepared by the classic metallographic process by polishing the samples with diamond pastes and etching them with an aqueous solution of ferric chloride.

3. RESULTS AND DISCUSSION

3.1. Thermodynamic calculation

Thermodynamic calculation of phase equilibria according to the CALPHAD (calculation of phase diagram) approach [19, 20] can provide valuable information about expected microstructure, phase transformation temperatures, and the thermal properties of the investigated material. In this work, thermodynamic calculations were performed using a thermodynamic dataset from Witusiewicz et al. [15]. Figure 1 presents a space phase diagram of the Bi-In-Sn system in combination with the constitutive In-Sn, Bi-Sn, and In-Bi binary systems.

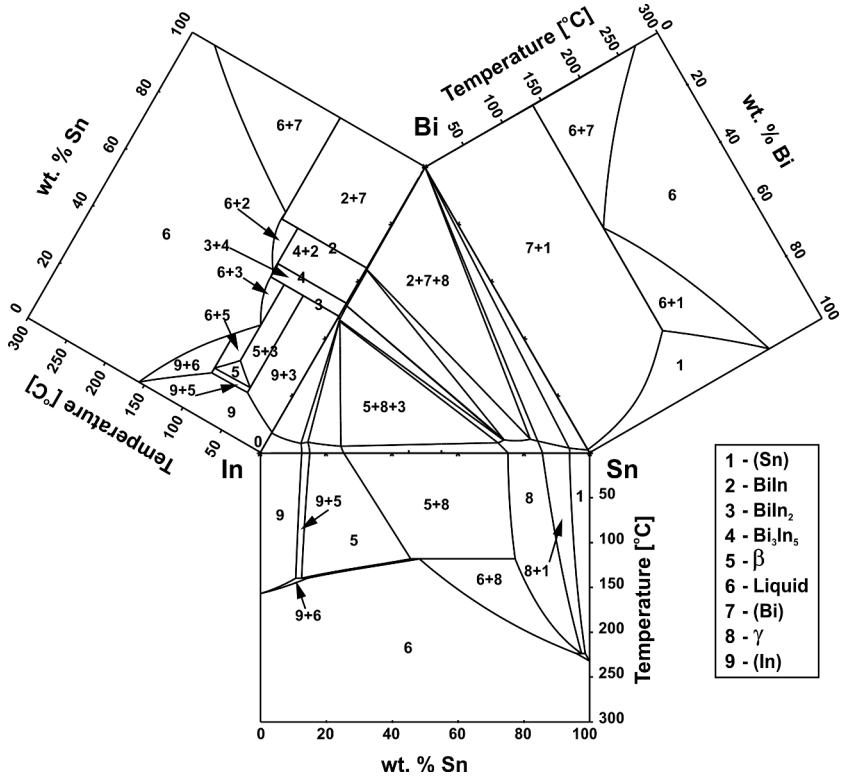

Figure 1. Space ternary phase diagram of Bi-In-Sn ternary system calculated using the thermodynamic parameters from Witusiewicz et al.[15]

Calculated isothermal section of the Bi-In-Sn system at room temperature, with marked phases and drawn compositions of the investigated alloys are shown in Figure 2.

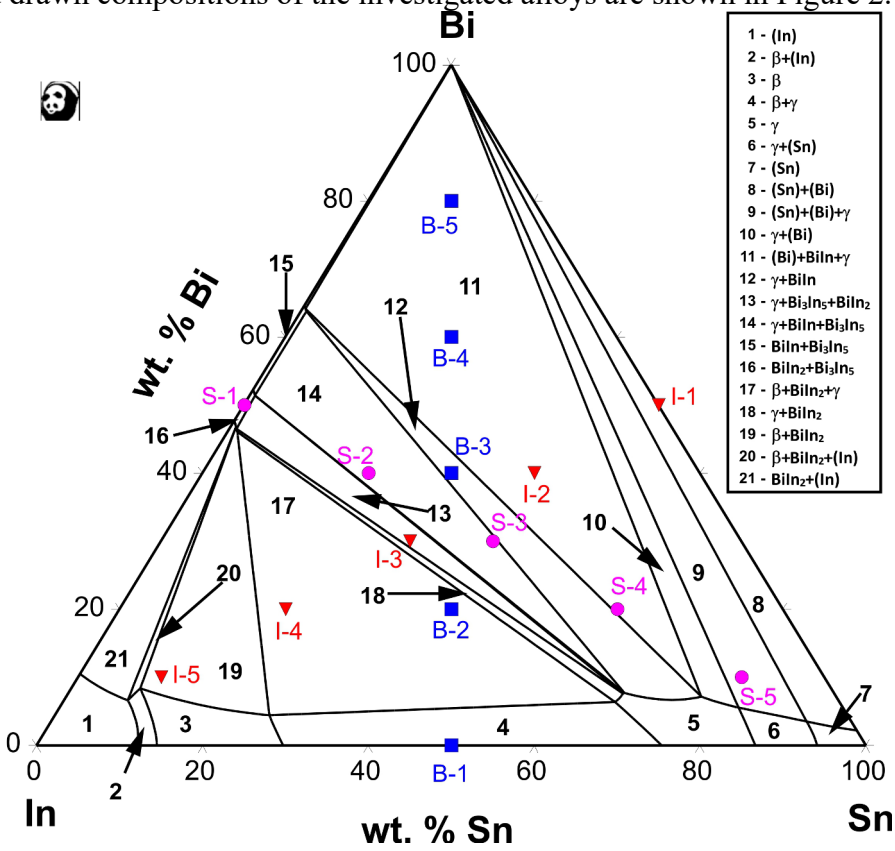

Figure 2. Calculated isothermal section of the Bi-In-Sn system at room temperature, based on thermodynamic parameters from Witusiewicz et al. [15] with marked phases and drawn compositions of the investigated alloys

3.2. Thermal analysis

Differential thermal analysis (DTA) was used to determine the melting temperature and temperature of phase transformations of the investigated alloys. Figure 3 shows examples of DTA heating curves for some of the tested alloys. It should be noted that the sample was heated twice to 300 °C in a nitrogen atmosphere with a heating rate of 10 °min^{-1}, and the results of the second heating are shown. The liquid temperature was determined from the temperature of the DTA peak while other phase transition temperatures were determined from the onset temperature of the DTA peak in the heating process.

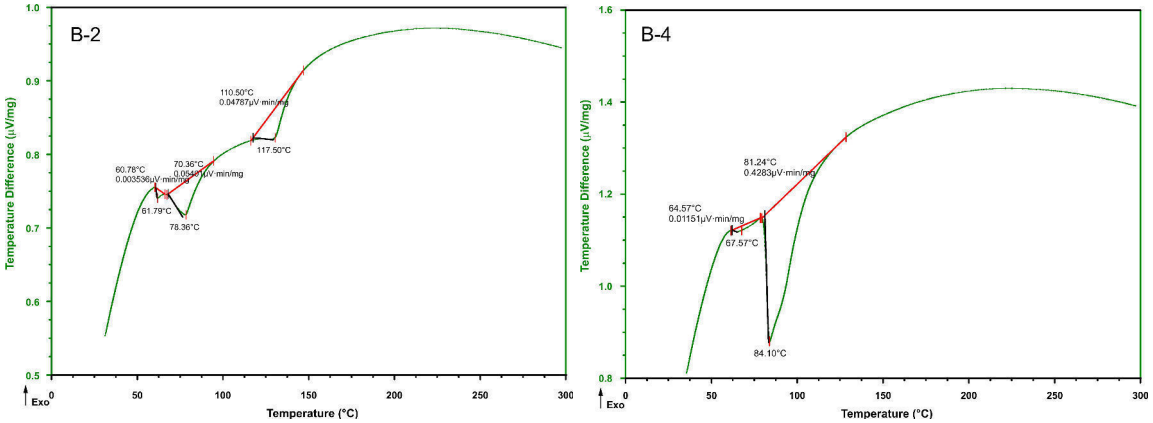

a) Investigated alloy B-2 and B-4 from Bi-Sn50In50 vertical section

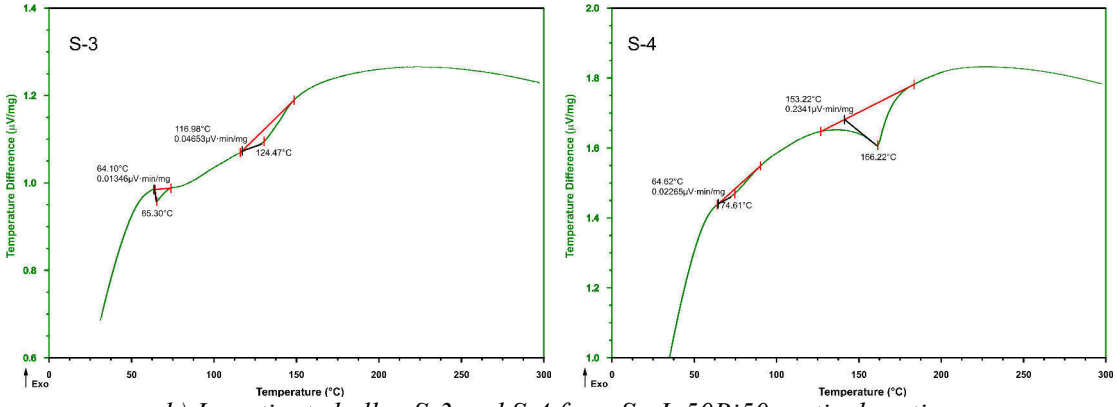

b) Investigated alloy S-3 and S-4 from Sn-In50Bi50 vertical section

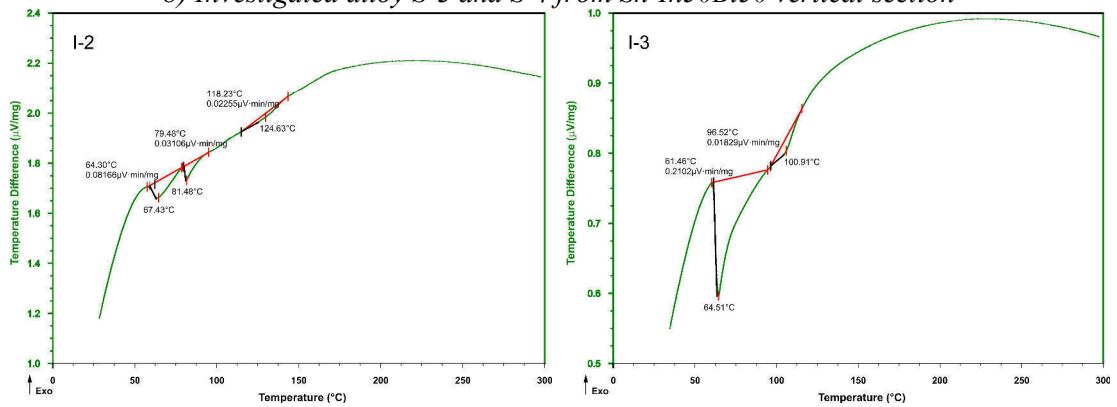

c) Investigated alloy I-2 and I-3 from In-Bi50Sn50 vertical section

Figure 3. DTA heating curve of investigated alloys from Bi-In-Sn ternary system

Experimentally determined temperatures of phase transformations in the investigated alloys of vertical sections Bi-Sn50In50, Sn-In50Bi50, and In-Bi50Sn50 are presented in Table 1. Figure 4 presents calculated vertical sections with mass fraction ratios In/Sn=1, Bi/Sn=1, and Bi/In=1 of the ternary Bi-In-Sn system compared with DTA experimental results: a) Bi-Sn50In50, b) Sn-In50Bi50 and c) In-Bi50Sn50. Experimentally determined temperatures of phase transformations of the investigated alloys were in good agreement with calculated values.

Table 1. Experimentally determined temperatures of phase transformations of the investigated alloys

Samples	Temperature, °C	
	Phase transformations	Liquidus
B-1	/	117,75
B-2	60,78; 70,36;	117,50
B-3	68,86	80,28
B-4	64,57	84,10
B-5	66,42; 85,32;	186,13
S-1	/	92,67
S-2	/	63,67
S-3	64,10	124,47
S-4	64,63	166,22
S-5	63,67	200,61
I-2	64,43; 79,48;	124,03
I-3	61,46	100,91
I-4	61,16	93,22
I-5	67,52	128,94

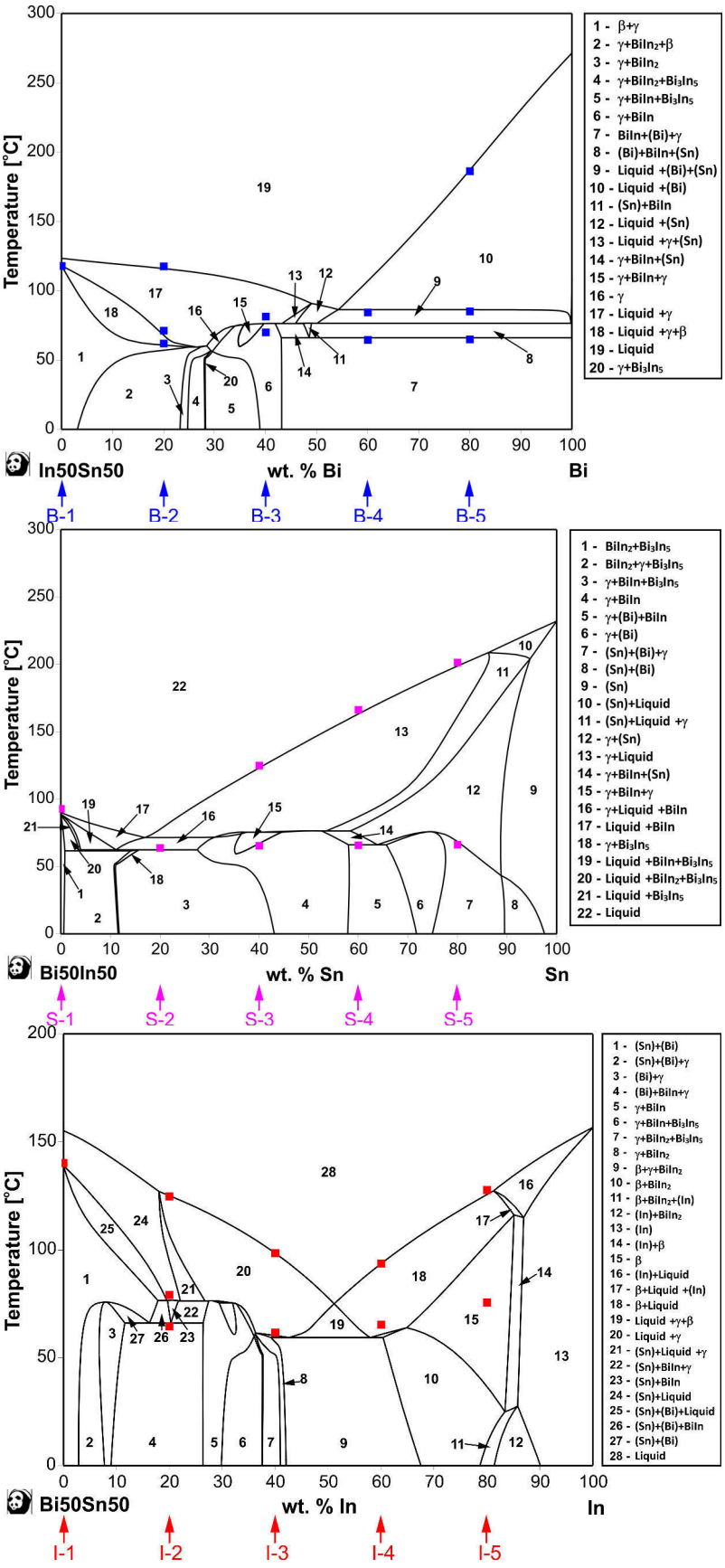

Figure 4. *Calculated vertical sections of the ternary Bi-In-Sn system, based on thermodynamic parameters from Witusiewicz et al. [15], compared with DTA experimental results: a) Bi-Sn50In50, b) Sn-In50Bi50 and c) In-Bi50Sn50*

3.3. Scanning Electron Microscopy (SEM-EDS)

The following images show SEM microphotographs of the investigated alloys B-2, B-3, and B-5 from Bi-Sn50In50 vertical section; S-2, S-3, and S-4 from Sn-In50Bi50 vertical section; I-3 and I-4 from In-Bi50Sn50 vertical section at different magnifications: a) 100x; b) 500x; c) 1000x; d) 2000x.

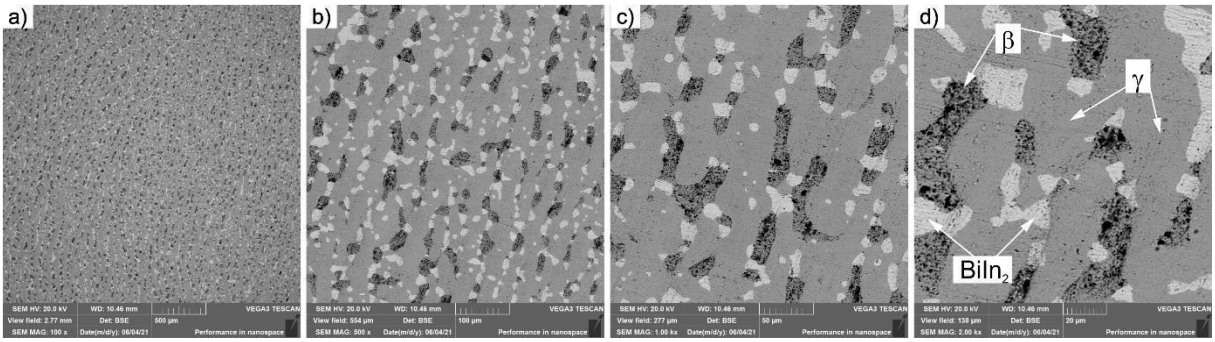

B-2

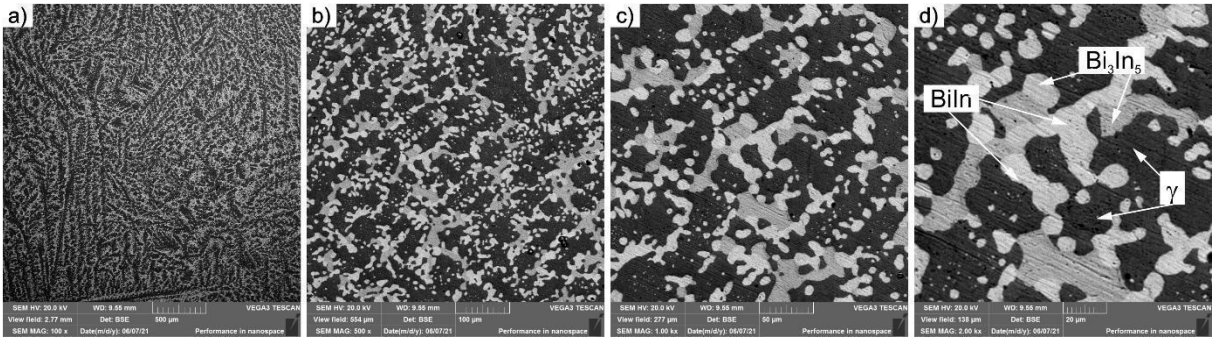

B-3

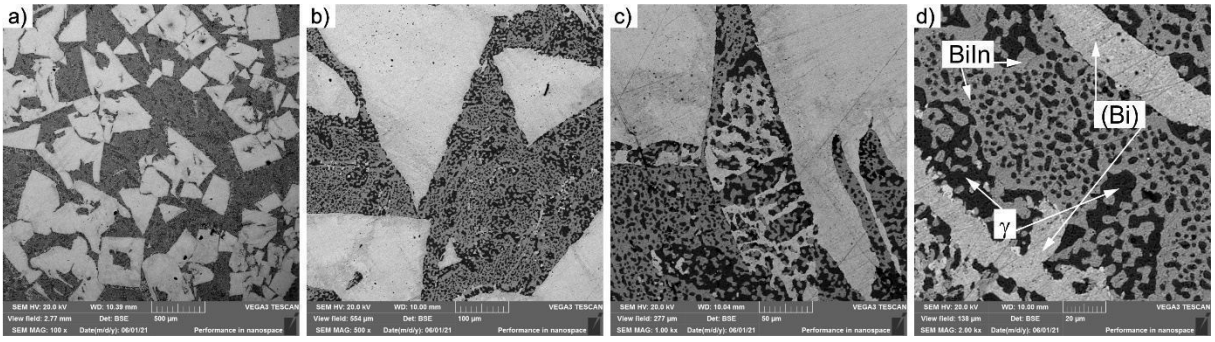

B-5

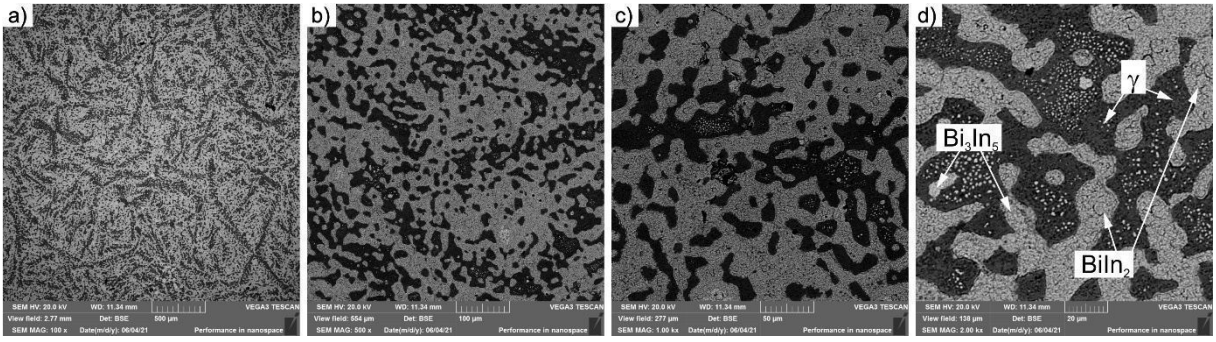

S-2

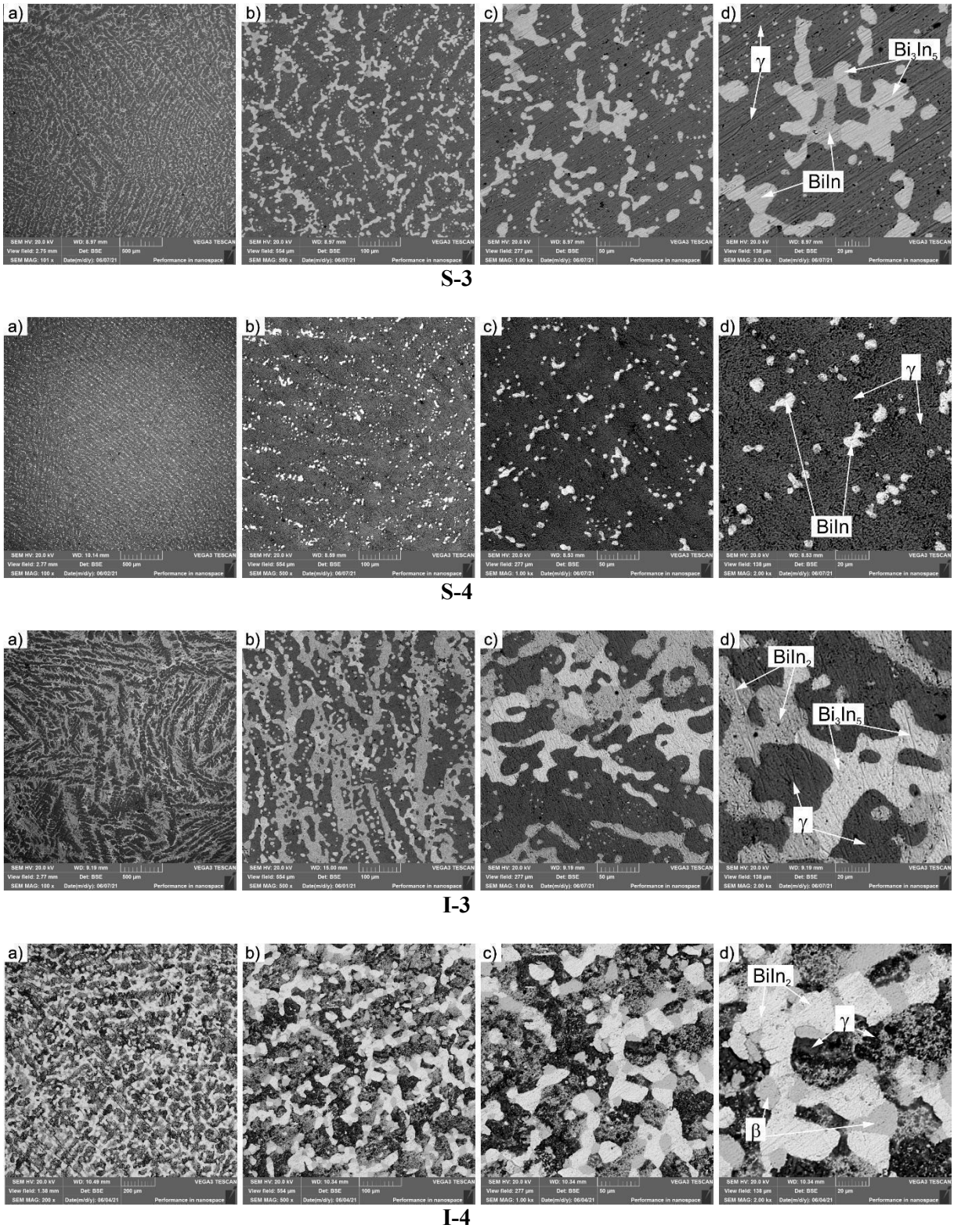

Figure 5. *SEM microphotographs of the investigated alloys B-2, B-3, and B-5 from Bi-Sn50In50 vertical section; S-2, S-3, and S-4 from Sn-In50Bi50 vertical section; I-3 and I-4 from In-Bi50Sn50 vertical section at different magnifications: a) 100x; b) 500x; c) 1000x; d) 2000x*

In SEM microphotographs of alloy B-2, it can be clearly seen that the microstructure consists of three phases: the largest dark gray phase is the γ phase, $BiIn_2$ is the light gray phase, and the black phase is the β phase. While in alloy B-3, the microstructure consists

of three phases: the largest black phase is the γ phase, the dark gray phase is BiIn, and the light gray phase is the Bi_3In_5 phase. The microstructure of alloy B-5 consists of three phases: the black phase is the γ phase, the light gray phase is a solid solution based on bismuth (Bi), and the dark gray phase is the BiIn phase. In the SEM microphotographs of the S-2 and S-3 alloys, the microstructure consists of three phases: the black phase is the γ phase, the light gray phase is Bi_3In_5 and the dark gray phase is $BiIn_2$ at the alloy S-2 and BiIn at the alloy S-3. The microstructure of S-4 alloys consists of only two phases: the black phase is the γ phase, and the light gray phase is BiIn, while the third phase, a solid solution based on bismuth (Bi), which should be present in this alloy, has not been identified. In the SEM microphotograph of the I-3 alloy, the base of the microstructure is the same black γ phase. Two more phases are present there. The light gray phase is the stoichiometric compound Bi_3In_5, and the dark gray phase is the same stoichiometric compound $BiIn_2$. In the case of I-4 alloys, the base of the microstructure is also the black γ phase. Two more phases are also present there. The light gray phase is the stoichiometric compound $BiIn_2$, and the dark gray phase is the β phase. Experimentally determined phase compositions of co-existing phases in the investigated alloys were found to support the corresponding calculated phase compositions based on thermodynamic parameters from Witusiewicz et al. [15], quite well.

4. CONCLUSIONS

In the present research, low-melting alloys from three cross-sections Bi-Sn50In50, Sn-In50Bi50, and In-Bi50Sn50 was investigated using differential thermal analysis (DTA), and by scanning electron microscopy (SEM) with energy dispersive spectrometry (EDS). Temperatures of phase transformations, determined by DTA, were compared with the calculated vertical sections (three vertical sections were investigated), and a close agreement was obtained. Phase compositions of co-existing phases, determined by EDS analysis, were found to support the corresponding calculated phase compositions quite well. The experimentally obtained results were compared with the results of thermodynamic calculation according to the CALPHAD (calculation of phase diagram) approach, based on thermodynamic parameters from Witusiewicz et al. [15], and a close agreement was noticed.

5. ACKNOWLEDGEMENT

This work has been financial supported by the Ministry of Science, Technological Development and Innovations of the Republic of Serbia, with the funding of the scientific research work at the University of Belgrade, Technical Faculty in Bor, according to the contract with registration number 451-03-47/2023-01/200131. The authors are grateful to V.T. Witusiewicz for kindly providing TDB file for thermodynamic calculations.

6. REFERENCES

[1] Said R.M., Salleh M.A.A.M., Saud N., Ramli M.I.I.: Superconducting Lead-free Solder Joint: A Short Review, IOP Conference Series: Materials Science and Engineering, Volume 957 (Issue 1), Pahang, Virtual; Malaysia, IOP Publishing Ltd, (2020)

[2] Cheng S., Huang C.-M., Pecht M.: A review of lead-free solders for electronics applications, Microelectronics Reliability, 75 (2017) 77-95

[3] Aksoy C., Mousavi T., Brittles G., Grovenor C.R.M., Speller S.C.: Lead-Free Solders for Superconducting Applications, IEEE Transactions on Applied Superconductivity, 26 (3) (2016)

[4] Kotadia H.R., Howes P.D., Mannan S.H.: A review: On the development of low melting temperature Pb-free solders, Microelectronics Reliability, 54 (6) (2014) 1253-1273

[5] Directive 2002/96/EC of the European parliament and of the council, on waste electrical and electronic equipment (WEEE), Official Journal of the European Union, L 37 (2003) 24-38
[6] Directive 2002/95/EC of the European parliament and of the council on the restriction of the use of certain hazardous substances in electrical and electronic equipment (RoHS), Official Journal of the European Union, L 37 (2003) 19-23
[7] Puttlitz K., Galyon G.: Impact of the ROHS directive on high-performance electronic systems Part I: need for lead utilization in exempt systems, Journal of Materials Science: Materials in Electronics, 18 (1) (2007) 331-346
[8] Puttlitz K., Galyon G.: Impact of the ROHS Directive on high-performance electronic systems Part II: key reliability issues preventing the implementation of lead-free solders, Journal of Materials Science: Materials in Electronics, 18 (1) (2007) 347-365
[9] Mhd. Noor E.E., Ismail A.B., Sharif N.M., Ariga T., Hussain Z.: Characteristic of low temperature of Bi-In-Sn solder alloy, Proceedings of the IEEE/CPMT International Electronics Manufacturing Technology (IEMT) Symposium, (2008)
[10] Yang F., Zhang L., Liu Z.Q., Zhong S.J., Ma J., Bao L.: Properties and Microstructures of Sn-Bi-X Lead-Free Solders, Advances in Materials Science and Engineering, 2016 (2016)
[11] Zhou K., Tang Z., Lu Y., Wang T., Wang H., Li T.: Composition, Microstructure, Phase Constitution and Fundamental Physicochemical Properties of Low-Melting-Point Multi-Component Eutectic Alloys, Journal of Materials Science & Technology, 33 (2) (2017) 131-154
[12] Yang C.H., Zhou S., Lin S.K., Nishikawa H.: Development of Sn-Bi-In-Ga quaternary low-Temperature solders, 2019 International Conference on Electronics Packaging, ICEP 2019, (2019)
[13] Shalaby R.M.: Effect of silver and indium addition on mechanical properties and indentation creep behavior of rapidly solidified Bi–Sn based lead-free solder alloys, Materials Science and Engineering: A, 560 (2013) 86-95
[14] Chen X., Xue F., Zhou J., Yao Y.: Effect of In on microstructure, thermodynamic characteristic and mechanical properties of Sn–Bi based lead-free solder, Journal of Alloys and Compounds, 633 (2015) 377-383
[15] Witusiewicz V.T., Hecht U., Böttger B., Rex S.: Thermodynamic re-optimisation of the Bi–In–Sn system based on new experimental data, Journal of Alloys and Compounds, 428 (1-2) (2007) 115-124
[16] Quezada-Castillo E., Aguilar-Castro W., Quezada-Alván B.: Ion release from non precious dental alloys in the oral cavity, Revista Materia, 27 (2) (2022)
[17] Mang S.R., Choi H., Lee H.J.: Investigation of Sn–Bi–In ternary solders with compositions varying from Sn–Bi eutectic point to 76 °C ternary eutectic, Journal of Materials Science: Materials in Electronics (2022)
[18] Peng Y., Li C., Xiao K., Yang J., Pu C., Gao P., Guo S., Zhang J., Yi J.: Effects of Ga alloying on microstructure and comprehensive performances of Sn–9Zn–2Bi alloys for the microelectronics industry, Microelectronics Reliability, 135 (2022)
[19] Saunders N., Miodownik A.P.: CALPHAD (CALculation of PHAse Diagrams): A comprehensive guide, New York, Pergamon, 1998
[20] Lukas H., Fries S.G., Sundman B.: Computational thermodynamics: the Calphad method, Cambridge university press, 2007